Quantifying the Regularity of Perturbed Triangular Lattices using CoV-Based Metrics for Modeling the Locations of Base Stations in HetNets

Faraj Lagum, Sebastian S. Szyszkowicz and Halim Yanikomeroglu
Department of Systems and Computer Engineering, Carleton University, Ottawa, Ontario, Canada.
Email: {faraj.lagum, sz, halim}@sce.carleton.ca

***Abstract*—In this paper, we give qualitative and quantitative arguments for the use of perturbed triangular lattice (PTL) models for generating base station deployments with any amount of spatial regularity, which is useful notably in modeling different tiers of HetNets. We use the coefficient of variation of three spatial properties of point processes to measure the regularity of two common types of PTL: uniform on disc and Gaussian. From these measurements, we are able to derive a simple formula that allows matching and interchanging the two PTL models, within about 0.1 dB error in SIR.**

***Index Terms*—Stochastic geometry; 5G; HetNets; hexagonal lattice; repulsive point process; regularity; second-order statistics.**

I. Introduction

In future networks, heterogeneous networks (HetNets) are expected to consist of multiple tiers of different types of base station (BS): macro, pico, and femto. These are expected to have not only different densities but also different deployment regularity [1], [2]. The performance of wireless cellular networks depends on the spatial deployment of the BSs because the received and interference signal powers depend on the distance between the transmitters and the receiver. Indeed, a BS deployment with high regularity has a better network performance than the one with low regularity [3], [4]. Therefore, modeling and analyzing the placement of BSs in wireless networks have drawn the attention of the researchers in both industry and academia in the recent years.

Most of the work on the evaluation of the network performance uses two extreme models for BSs placement: a triangular lattice (TL) at one end and a homogeneous Poisson point process (PPP) at the other end. These two models are extremes in terms of regularity and in terms of the network performance: While the TL modeling provides an optimistic network performance, the PPP is a pessimistic model. Indeed, the real deployment of BS locations probably lies somewhere between these two extremes [1], [4], [5].

Repulsive point processes (RPPs) have been widely investigated in the literature for modeling the BS locations because of their regularity property. The soft-core variety of RPPs used in wireless literature includes determinantal point process models [6], and the family of Gibbs point processes [4], [7]. In [3], we evaluated three hard-core point processes, the other variety of RPPs, for modeling BS locations: the Matern hard-core processes of type I and type II [8], [9], and the simple sequential inhibition (SSI) process [9]. All these RPPs are based on generating independent points, and then removing certain points based on some formula involving their mutual distances and sequential order. Therefore, one important limitation of these RPPs is their inability to provide very high regularity [3], [4], as it is not possible to obtain a TL from thinning a PPP. It is also often necessary to generate a large number of points (and evaluate the distance between each pair), in order to obtain a smaller number of points at the output, making these methods computationally costly.

In order to overcome these limitations, we advocate the use of the perturbed triangular lattice (PTL), which can be tuned over the whole range between the deterministic TL and the PPP [5], [7], for modeling the multi-tier BSs in HetNets. The PTL can be scaled with different densities for different simulation scenarios without changing the regularity of the deployment. Recently, the uniform PTL is found to be tractable in [5]. The PTL is also a simple model to simulate; as a consequence, it is practical and widely used in the industry [7].

Motivation: One of the challenges in BS location modeling is how to adjust the internal parameters of different models to produce spatial patterns with the same amount of regularity, or to check whether two given spatial patterns are similar or not. The first step to overcome this challenge is to find good metrics for the regularity of a spatial pattern in order to precisely define where it lies between the TL and the PPP. We used three CoV-based metrics in [3] to quantify the regularity of hard-core point processes for modeling for BS locations; these metrics were originally proposed in [10] for measuring the attraction in clustered point processes for modeling user locations. The second step, which is the focus of this paper, is to use these metrics as an intermediate stage to map different models to each other.

Contribution: The main contribution of this paper is proposing a novel approach for mapping between different RPPs using CoV-based metrics. Specifically, we find a simple and accurate formula for mapping between the uniform PTL and the Gaussian PTL. We show that the CoV-based metrics are suitable for quantifying the regularity of PTL lattice models. Similarly to our previous work [3], where we found that different hard-core models with the same CoV-based metric value and density have very similar network performance, here we show that this is true for different PTLs as well.

The rest of this paper is organized as follows: In Section II, perturbed triangular lattice models are introduced. In Section III, CoV-based metrics are presented. n Section IV, we measured the regularity of the perturbed triangular lattices using the CoV-based metrics to quantify regularity. We proposed new a approach using the CoV-based metrics for mapping between two PTL models in Section V. Finally, we draw the conclusions in Section VI.

II. Perturbed Triangular Lattices Models for Base Stations Placement

In the cellular network context, the triangular lattice is often used to model the layout of BSs. It is sometimes also called the hexagonal lattice because its Voronoi tessellation produces hexagonal cells. The PTL is a result of the independent random displacement of each point from its original location. In this section, we present two kinds of the perturbed triangular lattices: Gaussian PTL and uniform PTL.

Triangular Lattice: Beginning with a unit square lattice with integer coordinates $(a, b) \in \mathbb{Z}^2$, a triangular lattice can be produced by transforming the points using the generator matrix $G = \begin{bmatrix} 1 & 0 \\ \frac{1}{2} & \frac{\sqrt{3}}{2} \end{bmatrix}$ and scaling the coordinates by a factor η, which is the distance between any two nearest neighbour points. The TL has points with coordinates

$$\left\{ \left(\eta a + \tfrac{1}{2}\eta b, \tfrac{\sqrt{3}}{2}\eta b \right), (a, b) \in \mathbb{Z}^2 \right\}. \tag{1}$$

The TL has density $\lambda = \frac{1}{\det(G)}\eta^{-2} = \frac{2}{\sqrt{3}}\eta^{-2}$.

Stationary Triangular Lattice: Translation of all the lattice points by a common vector $(s_{\mathrm{x}}, s_{\mathrm{y}})$ uniformly distributed over the Voronoi cell of the origin point $(0, 0)$ results in a stationary point process [4]. For the triangular lattice, the Voronoi cell is a regular hexagon[1] with two vertical sides, centred at the origin with side length $\eta/\sqrt{3}$. The stationary triangular lattice has coordinates

$$\left\{ \left(\eta a + \tfrac{1}{2}\eta b + s_{\mathrm{x}}, \tfrac{\sqrt{3}}{2}\eta b + s_{\mathrm{y}} \right), (a, b) \in \mathbb{Z}^2 \right\}, \tag{2}$$

where $(s_{\mathrm{x}}, s_{\mathrm{y}})$ is uniformly distributed over the aforementioned hexagon. All PTL models are assumed to be stationary in this paper.

Perturbed Triangular Lattices: For any perturbed lattice, each point is independently displaced by random vector $\left(x_{(a,b)}, y_{(a,b)}\right)$ [9]. The PTL has coordinates

$$\left\{ \left(\eta a + \tfrac{1}{2}\eta b + s_{\mathrm{x}} + x_{(a,b)}, \tfrac{\sqrt{3}}{2}\eta b + s_{\mathrm{y}} + y_{(a,b)} \right), (a, b) \in \mathbb{Z}^2 \right\}, \tag{3}$$

where $\left\{ \left(x_{(a,b)}, y_{(a,b)}\right) \right\}$ is a set of independent and identically distributed vectors. The distribution from which the vectors are drawn characterizes the type of PTL.

In this paper, we study two kinds of perturbation: Gaussian and uniform. The uniform PTL is one where the displacement vectors are uniformly distributed over a disc of radius R, which controls the amount of perturbation, and can be normalized as $\tilde{R} = R\eta^{-1}$ to be independent of the density. Similarly, the Gaussian PTL is one where the displacement coordinates $x_{(a,b)}$ and $y_{(a,b)}$ are each taken independently from a Gaussian distribution with mean 0 and standard deviation σ, which controls the amount of perturbation, and can be normalized as $\tilde{\sigma} = \sigma\eta^{-1}$ to be independent of the density.

An interesting observation about the uniform perturbation on a disc is that the model can work either as a soft-core or as a hard-core model depending on the perturbation regime. It is a hard-core model in the regime $\tilde{R} < 0.5$ (the hard-core distance is then $h = (1 - 2\tilde{R})\eta$), and it is a soft-core model after that. The Gaussian PTL is always a soft-core model.

III. CoV-Based Metrics

The CoV of a random variable is defined as its standard deviation normalized by its mean. The CoVs of three geometric properties of point processes have been introduced in [10] as metrics of the clustering of mobile user locations, and we have used these metrics in [3] to measure the regularity of hard-core RPPs for modeling BS locations. Each CoV metric was further normalized by a constant factor so that its value would always be 1 for the PPP. All three CoV-based metrics take the value of 0 for the TL, and increase as the process becomes less regular. Values above 1 are found for clustered point processes [10], which are not considered in this work.

a) CoV of the Distances to the Nearest Neighbour: For every point in the RPP, find its nearest neighbour and measure the distance to it [11]. The CoV-based metric is then

$$C_{\mathrm{N}} = \frac{1}{k_{\mathrm{N}}} \cdot \frac{\sigma_{\mathrm{N}}}{\mu_{\mathrm{N}}}, \qquad k_{\mathrm{N}} = \sqrt{\frac{4 - \pi}{\pi}} \cong 0.5227, \tag{4}$$

where μ_{N} is the mean and σ_{N} is the standard deviation of the nearest neighbour distances; and k_{N} is the normalization factor derived[2] from [11].

b) CoV of the Areas of Voronoi Tessellation Cells: Consider the Voronoi tessellation [9], [10] of a set of points (see Fig. 1), and measure the area of each Voronoi region. The CoV-based metric is then

$$C_{\mathrm{V}} = \frac{1}{k_{\mathrm{V}}} \cdot \frac{\sigma_{\mathrm{V}}}{\mu_{\mathrm{V}}}, \qquad k_{\mathrm{V}} \cong 0.529, \tag{5}$$

where μ_{V} is the mean and σ_{V} is the standard deviation of the Voronoi cell areas, and k_{V} is the normalization factor [10].

c) CoV of the Lengths of Delaunay Triangulation Edges: Consider the Delaunay triangulation [9], [10] of a set of points (see Fig. 1), and measure the length of each edge of the resulting graph. The CoV-based metric is then

$$C_{\mathrm{D}} = \frac{1}{k_{\mathrm{D}}} \cdot \frac{\sigma_{\mathrm{D}}}{\mu_{\mathrm{D}}}, \qquad k_{\mathrm{D}} \cong 0.492, \tag{6}$$

where μ_{D} is the mean and σ_{D} is the standard deviation of the Delaunay edge lengths, and k_{D} is the normalization factor [10].

The metrics C_{V}, C_{D}, and C_{N} are unit-less and are therefore invariant under scaling of the measured RPP, and are thus independent of the RPP's density λ.

[1] It is simpler to generate a stationary square lattice, where the Voronoi cell is a square, and then transform it into a stationary triangular lattice using the generator matrix G.

[2] In [10], the value for k_{N} is erroneously given as 0.653.

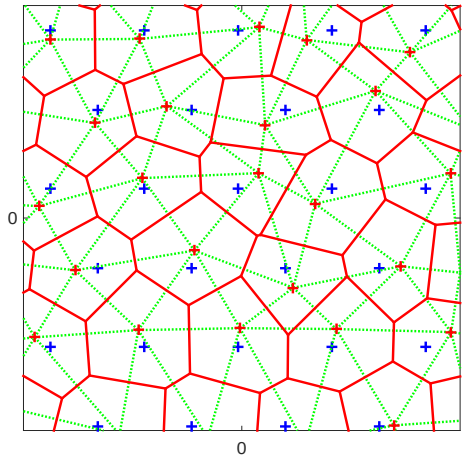

Fig. 1. Delaunay triangulation (green dashed lines) and Voronoi tessellation (red solid lines) of a spatial pattern (red plus marks) generated by uniform perturbation (with $\tilde{R} = 0.325$) of a triangular lattice (blue plus marks).

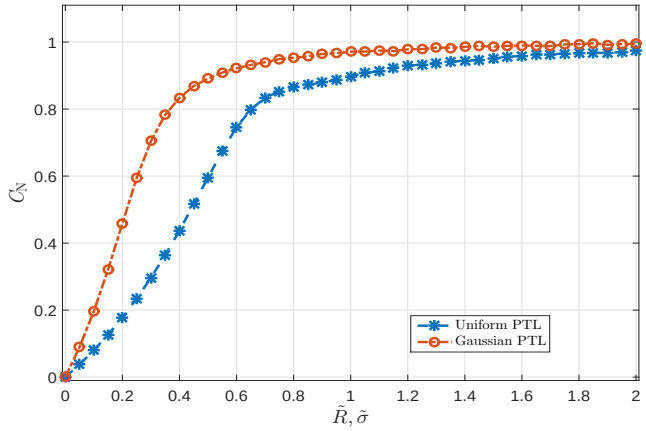

Fig. 2. The normalized CoV of the distance to the nearest neighbour as a function of the normalized perturbations.

IV. Measuring the Regularity of Perturbed Lattices

In this section, we consider a wireless cellular network with the BS placement modeled by the two PTL models introduced in Section II. The normalized parameters, $\tilde{R}$ for uniform PTL and $\tilde{\sigma}$ for Gaussian PTL, are swept from 0 to 2 in order to change the regularity of the models. For each model, we measure the amount of regularity using the three CoV-based metrics introduced in Section III. For each particular $\tilde{R}$ and $\tilde{\sigma}$ values, we perform a Monte-Carlo simulation with 1000 realizations, each with 500 BSs placed over a $1\,\mathrm{km}^2$ square area. The CoV-based metrics as a function of $\tilde{R}$ and $\tilde{\sigma}$ are shown in Figs. 2, 3, and 4.

As the perturbation parameters increase, the CoV-based metrics converge to 1 and the two models converge to the PPP. In other words, both models are able to span the whole range between the TL ($C_{\mathrm{N}} = C_{\mathrm{V}} = C_{\mathrm{D}} = 0$) and, asymptotically, the PPP ($C_{\mathrm{N}}, C_{\mathrm{V}}, C_{\mathrm{D}} \to 1$). A particular spatial pattern has different C_{N}, C_{V}, and C_{D} values. Fig. 5 shows the parametric curves of the relationships between the CoV-based metrics.

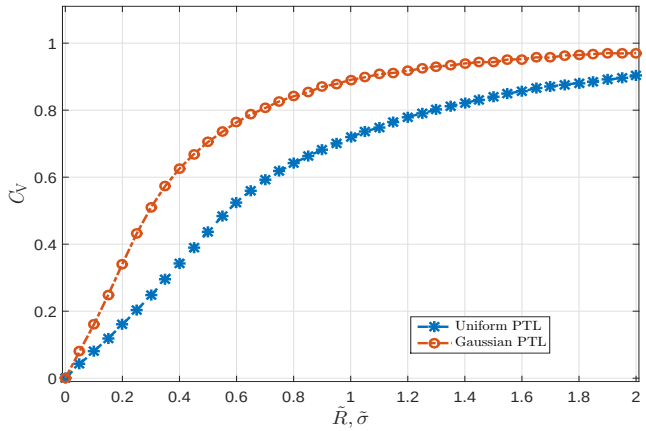

Fig. 3. The normalized CoV of the areas of the Voronoi tessellation cells as a function of the normalized perturbations.

V. Mapping Between Uniform PTL and Gaussian PTL Models Using the CoV-Based Metrics

A. Mapping

In a novel framework, we use the CoV-based metrics as an intermediate step for mapping between the uniform PTL and the Gaussian PTL. Using the simulation results from the previous section, for each CoV-based metric at a particular value, we find the corresponding internal parameter values $\tilde{R}$ and $\tilde{\sigma}$, for the uniform PTL model and the Gaussian PTL model, respectively. Parametrized curves describing the relationship between $\tilde{R}$ and $\tilde{\sigma}$ using the three CoV-based metrics are shown in Fig. 6. We find a good approximate fitting for all the three parametrized curves to be

$$\tilde{\sigma} \approx 0.53\tilde{R}. \tag{7}$$

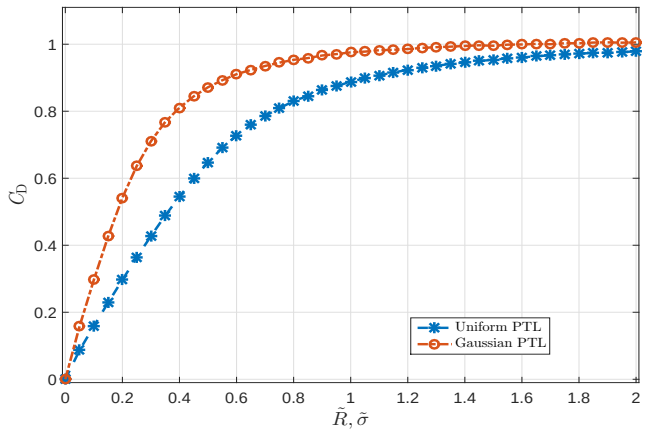

Fig. 4. The normalized CoV of the lengths of the Delaunay triangulation edges as a function of the normalized perturbations.

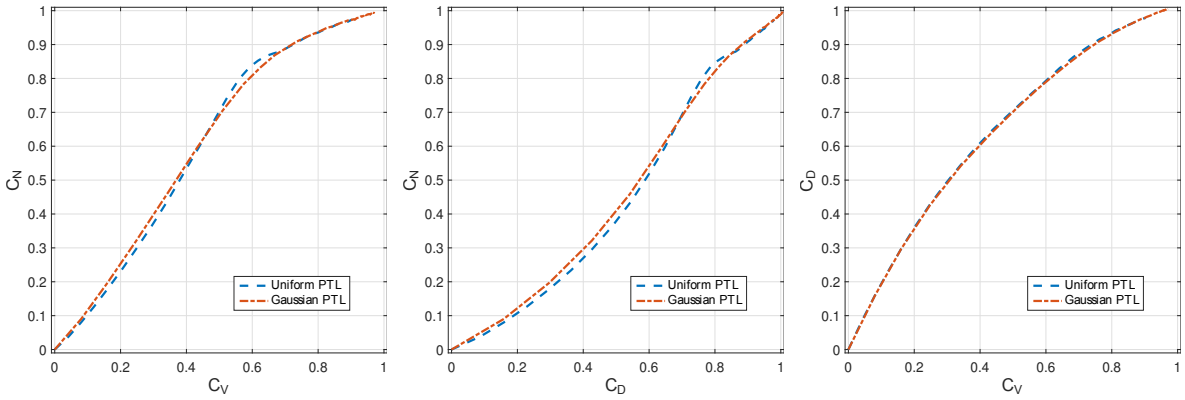

Fig. 5. The relationship between different CoV-based metrics of different PTL models.

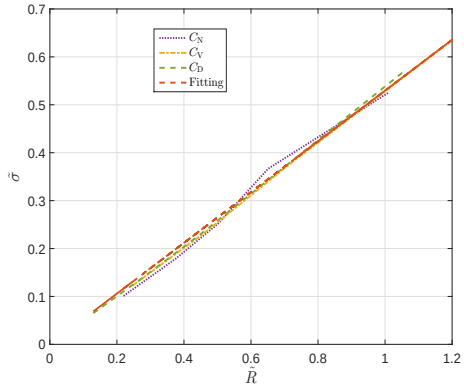

Fig. 6. The relationship between $\tilde{R}$ and $\tilde{\sigma}$ that gives equal CoV-metrics value.

This means that a spatial pattern generated by the uniform PTL with any perturbation value $\tilde{R}$ is almost equivalent in terms of regularity to another spatial pattern generated by the Gaussian PTL with perturbation value $\tilde{\sigma} = 0.53\tilde{R}$. Moreover, the two spatial patterns – when they are used to model BS locations – are also almost equivalent in terms of the network performance, as we will show in the next subsection.

B. Downlink Coverage Probability

We now validate that a pair of spatial patterns generated by uniform PTL and Gaussian PTL have similar network performance and regularity (as measured using the CoV-based metrics) if their internal parameters are simultaneously adjusted according to (7). A useful wireless network metric that we use to compare the network performance of different spatial deployments of BSs is the downlink coverage probability $P(\gamma)$, which is the probability that a typical user's signal-to-interference ratio (SIR) exceeds a threshold γ.

We consider a 100 macro BS (one tier) wireless network placed over a $1\,\mathrm{km}^2$ square area with simple network setup assumptions as follows. We consider two path-loss models: one with path-loss exponent $\alpha = 3$ and lognormal shadowing of $X_g = 6$ dB, and the other with $\alpha = 4$ and $X_g = 0$ dB. We will refer to these two path-loss models in Table I as CH1 and CH2, respectively. All the BSs transmit identical power, operate at the same frequency (the frequency reuse factor is 1), and are equipped with one antenna. 1000 mobile users are uniformly distributed over the network region. Each user is associated with its nearest serving BS. All the links experience independent Rayleigh fading with mean 1. We ignore the thermal noise. We use a simple network setup, similarly to [4], because our emphasis is on the validation of the mapping between the two PTL models.

Fig. 7 shows that uniform PTL and Gaussian PTL have similar downlink coverage probability when their parameters are matched according to (7). Fig. 7 also shows that the coverage probability curves of the PPP and TL represent the lower and the upper network performance bounds, respectively. Figs. 8 and 9, each for a specific path-loss model, show in detail the difference between the coverage probability curves and the PPP coverage probability curve. This SIR difference is the *deployment gain* defined in [4, Def. 9]. Table I summarizes the comparison between the two PTL models matched according to (7). The gap $\Delta\mathrm{SIR}_{50\%}$ is the dB difference in SIR between the coverage probability curves of the matched uniform PTL and the Gaussian PTL at a coverage probability of 50%. The matched models have similar CoV-based metrics values and negligible $\Delta\mathrm{SIR}_{50\%}$ for the two path-loss models. In fact, the difference in SIR between the matched uniform and Gaussian PTL is never much more than 0.1 dB.

VI. Conclusion

We proposed a novel approach for mapping between uniform PTL and Gaussian PTL using CoV-based metrics as an intermediate step. After measuring the regularity of PTL models using three metrics, we found a simple relation between the internal parameters of these two PTL models in order to generate two very similar spatial processes in terms of regularity and network performance. Therefore, considering only one type of PTL is enough since the other shows very similar performance.

This work advocates modeling the placement of different

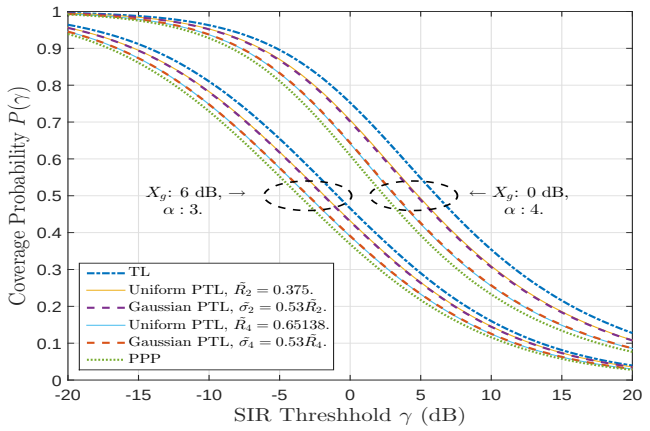

Fig. 7. The coverage probability for different PTL models for different perturbation values and channel environments.

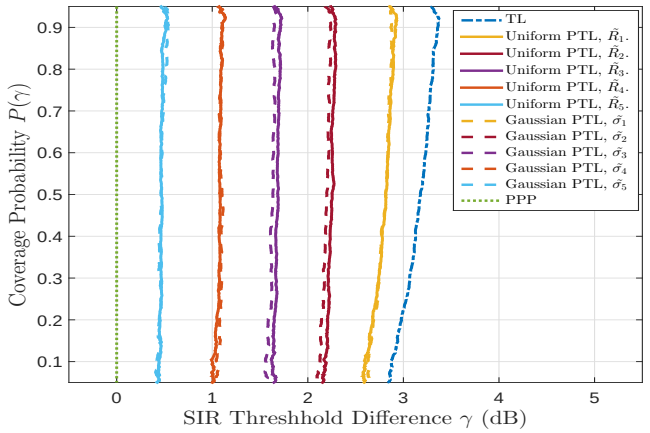

Fig. 8. The difference in SIR between the coverage probability of different spatial patterns and the PPP coverage probability. Path-loss model $\alpha = 3$ and $X_g = 6$ dB.

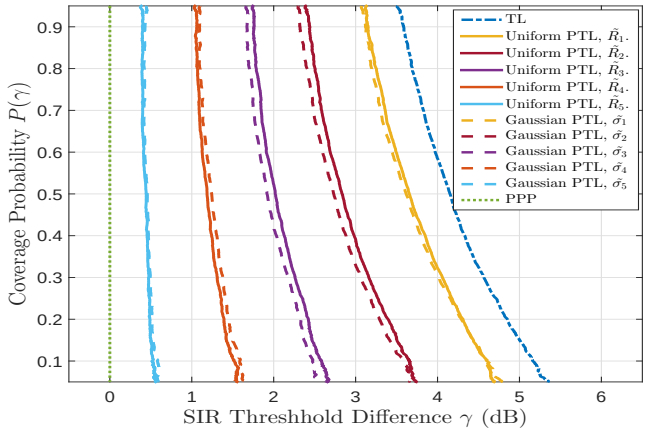

Fig. 9. The difference in SIR between the coverage probability of different spatial patterns and the PPP coverage probability. Path-loss model $\alpha = 4$ and $X_g = 0$ dB.

TABLE I
SUMMARY OF THE COMPARISON BETWEEN THE MATCHED UNIFORM PTL AND GAUSSIAN PTL.

	i	1	2	3	4	5
Uniform PTL	$\tilde{R}_i$	0.219	0.375	0.503	0.651	1.000
	C_{N}	0.201	0.401	0.600	0.800	0.898
	C_{V}	0.177	0.318	0.440	0.561	0.720
	C_{D}	0.323	0.517	0.650	0.760	0.888
Gaussian PTL $\tilde{\sigma}_i = 0.53\tilde{R}_i$	$\tilde{\sigma}_i$	0.116	0.198	0.266	0.345	0.530
	C_{N}	0.236	0.456	0.634	0.777	0.902
	C_{V}	0.188	0.339	0.459	0.568	0.724
	C_{D}	0.341	0.539	0.663	0.763	0.885
$\Delta\mathrm{SIR}_{50\%}$ [dB]	CH1	-0.003	0.055	0.051	-0.023	0.003
	CH2	0.038	0.104	0.101	-0.057	-0.013

types of BSs in HetNets using one of the PTL models, because of their simple and efficient implementation, their full regularity range (from the TL to the PPP), and their prevalence in industry and in recent wireless literature.

Future work could involve fitting real BS location data to RPP models using CoV-based metrics, as well as fitting different types of RPP models to each other. Ultimately, we would like to describe the spatial structure of any wireless network using only two scalars: the density of the BSs and a regularity metric value.

ACKNOWLEDGEMENTS

This work is funded in part by TELUS, Canada, and in part by the Ministry of Higher Education and Scientific Research (MOHESR), Libya, through the Libyan-North American Scholarship Program.

REFERENCES

[1] J. Andrews, "Seven ways that HetNets are a cellular paradigm shift," *IEEE Commun. Mag.*, vol. 51, no. 3, pp. 136–144, Mar. 2013.

[2] Y. J. Chun, M. O. Hasna, A. Ghrayeb, and M. Di Renzo, "On modeling heterogeneous wireless networks using non-poisson point processes," *IEEE Commun. Mag.*, pp. 1–7, June 2015, submitted. [Online]. Available: http://arxiv.org/abs/1506.06296

[3] F. Lagum, S. Szyszkowicz, and H. Yanikomeroglu, "CoV-Based Metrics for Quantifying the Regularity of Hard-Core Point Processes for Modeling Base Station Locations," *IEEE Wireless Commun. Lett.*, vol. 5, no. 3, pp. 276–279, June 2016.

[4] A. Guo and M. Haenggi, "Spatial stochastic models and metrics for the structure of base stations in cellular networks," *IEEE Trans. Wireless Commun.*, vol. 12, no. 11, pp. 5800–5812, Nov. 2013.

[5] S. A. Banani, R. S. Adve, and A. W. Eckford, "A perturbed hexagonal lattice to model basestation locations in real-world cellular networks," in *2015 IEEE Globecom Workshops*, Dec. 2015, pp. 1–6.

[6] Y. Li, F. Baccelli, H. Dhillon, and J. Andrews, "Fitting determinantal point processes to macro base station deployments," in *IEEE Global Commun. Conference (GLOBECOM)*, Dec. 2014, pp. 3641–3646.

[7] D. Taylor, H. Dhillon, T. Novlan, and J. Andrews, "Pairwise interaction processes for modeling cellular network topology," in *IEEE Global Commun. Conference (GLOBECOM)*, Dec. 2012, pp. 4524–4529.

[8] M. Haenggi, "Mean interference in hard-core wireless networks," *IEEE Commun. Lett.*, vol. 15, no. 8, pp. 792–794, Aug. 2011.

[9] ——, *Stochastic Geometry for Wireless Networks*. Cambridge University Press, 2012.

[10] M. Mirahsan, R. Schoenen, and H. Yanikomeroglu, "HetHetNets: Heterogeneous traffic distribution in heterogeneous wireless cellular networks," *IEEE J. Sel. Areas Commun.*, vol. 33, no. 10, pp. 2252–2265, Oct. 2015.

[11] P. M. Dixon, "Nearest neighbor methods," *Encyclopedia of Environmetrics*, 2002.